DØ note 5437-CONF

Simultaneous measurement of $\mathcal{B}(\mathbf{t \to Wb})/\mathcal{B}(\mathbf{t \to Wq})$ and $\sigma(\mathbf{p\bar{p} \to t\bar{t}})$ at DØ

The DØ Collaboration
URL http://www-d0.fnal.gov

(Dated: July 18, 2007)

We present the simultaneous measurement of the ratio of branching fractions R= $\mathcal{B}(t \to Wb)/\mathcal{B}(t \to Wq)$ and the top quark pair ($t\bar{t}$) production cross section ($\sigma_{t\bar{t}}$) in $p\bar{p}$ collisions at $\sqrt{s} = 1.96$ TeV, using about 900 pb^{-1} of data collected by the DØ experiment at the Fermilab Tevatron Collider. We select events with one charged lepton ℓ (electron or muon), missing transverse energy ($\not\!\!E_T$), and at least three jets in the final state. We use a lifetime-based b-jet identification technique to count the number of ℓ+jets+$\not\!\!E_T$ events with 0, 1 and at least 2 b-jets. A likelihood discriminant based on the kinematic properties of $t\bar{t}$ events is used to further constrain the number of $t\bar{t}$ events without tagged jets. For the top quark mass of 175 GeV we measure:

$$\begin{aligned} R &= 0.991^{+0.094}_{-0.085}\ \text{(stat+syst)}\ , \\ \sigma(t\bar{t}) &= 8.10^{+0.87}_{-0.82}\ \text{(stat+syst)} \pm 0.49\ \text{(luminosity) pb}\ , \end{aligned}$$

in good agreement with the standard model expectation. We set a lower limit of $R > 0.812$ at 95% C.L.

I. INTRODUCTION

The CKM matrix element $|V_{tb}|$ is indirectly constrained by the measurement of other CKM matrix elements to the interval $0.9990 < |V_{tb}| < 0.9992$ at the 90% C.L. [1], based on the assumption of unitarity of the CKM matrix. In this case the ratio of branching fractions $R = \mathcal{B}(t \to Wb)/\mathcal{B}(t \to Wq)$, where q is d, s or b, can be expressed in terms of CKM matrix elements:

$$R = \frac{|V_{tb}|^2}{|V_{tb}|^2 + |V_{ts}|^2 + |V_{td}|^2} = |V_{tb}|^2. \quad (1)$$

In the framework of the standard model (SM), the ratio R is therefore constrained to be in the interval 0.9980-0.9984 at the 90% C.L. [1]. If, for example, a fourth quark generation exists, the 3×3 standard model CKM matrix would appear non-unitary.

Until now three independent measurements of R performed under the assumption that the top quark decays only through the W boson exist. The CDF collaboration has measured $R = 0.94^{+0.31}_{-0.24}$ (stat + syst) and a lower limit $R > 0.56$ at 95% C.L. in Run I [2] with 109 pb^{-1} of integrated luminosity, and $R = 1.12^{+0.27}_{-0.23}$ (stat + syst) and a lower limit $R > 0.61$ at 95% C.L. in Run II [3] with 162 pb^{-1} of integrated luminosity. The DØ Collaboration has measured $R = 1.03^{+0.19}_{-0.17}$ (stat + syst) and a lower limit $R > 0.61$ at 95% C.L. in Run II [4] using an integrated luminosity of 230 pb^{-1}. All three measurements show consistency with the Standard Model prediction. Due to a larger integrated luminosity of 900 pb^{-1} and improvements in b-jet identification and the analysis method we expect a more precise result for R in this analysis.

Experimentally, R can be determined by selecting a sample enriched in $t\bar{t}$ events. The selected events are categorized into events with 0, 1 and 2 or more b-tagged jets. From the distribution of the observed events between the three categories and the kinematics of events without b-tagged jet, R and the $t\bar{t}$ pair production cross section can be extracted simultaneously.

In this paper, we report the measurement of $\mathcal{B}(t \to Wb)/\mathcal{B}(t \to Wq)$ and $\sigma_{t\bar{t}}$ in the lepton (electron or muon) plus jets channel using b-jet identification (b-tagging) techniques exploiting the long lifetime of B hadrons. The data were collected by the DØ experiment from August 2002 through December 2005, and correspond to an integrated luminosity of 912 ± 56 pb^{-1} (871 ± 53 pb^{-1}) in the electron (muon) sample. Similar to the previous measurements of R we assume that $\mathcal{B}(t \to Wq) = 1$.

II. DØ DETECTOR

The DØ detector includes a tracking system, calorimeters, and a muon spectrometer [5]. The tracking system consists of a silicon microstrip tracker (SMT) and a central fiber tracker (CFT), both located inside a 2 T superconducting solenoid. The tracker design provides efficient charged particle measurements in the pseudorapidity [6] region $|\eta| < 3$. The SMT strip pitch of 50–80 μm allows a precise reconstruction of the primary interaction vertex (PV) and an accurate determination of the impact parameter of a track relative to the PV [7], which are the key components of the lifetime-based b-jet tagging algorithms. The PV is required to be within the SMT fiducial volume and consist of at least 3 tracks. The calorimeter consists of a central section (CC) covering $|\eta| < 1.1$, and two end calorimeters (EC) extending the coverage to $|\eta| \approx 4.2$. The muon system surrounds the calorimeter and consists of three layers of tracking detectors and two layers of scintillators [8]. A 1.8 T iron toroidal magnet is located outside the innermost layer of the muon detector. The luminosity is calculated from the rate for $p\bar{p}$ inelastic collisions detected using two hodoscopes of scintillation counters mounted close to the beam pipe on the front surfaces of the EC calorimeters.

III. EVENT PRESELECTION

To select data samples in the electron and muon channels, we require an isolated electron with $p_T > 20$ GeV and $|\eta| < 1.1$, or an isolated muon with $p_T > 20$ GeV and $|\eta| < 2.0$. More details on the lepton identification as well as trigger requirements are reported elsewhere [9]. In the electron (muon) channel we require $\not\!\!E_T$ to exceed 20 GeV (25 GeV). We require $\not\!\!E_T$ to be non-collinear with the lepton direction in the transverse plane. These W boson candidate events must be accompanied by one or more jets with $p_T > 20$ GeV, the leading jet with $p_T > 40$ GeV, and rapidity $|y| < 2.5$ [6]. Jets are defined using a cone algorithm with radius $\sqrt{((\Delta\eta)^2 + (\Delta\phi)^2)} = 0.5$ [11]. The selected events are classified according to their jet multiplicity. Events with ≥ 3 jets are expected to be enriched in $t\bar{t}$ signal, whereas events with only 1 or 2 jets are expected to be dominated by background. We use the former to estimate $\mathcal{B}(t \to Wb)/\mathcal{B}(t \to Wq)$ and $\sigma_{t\bar{t}}$, and the latter to verify the background normalization procedure.

The main background in this analysis is the production of W bosons in association with jets (W+jets), with the W boson decaying leptonically. In most cases, the jets accompanying the W boson originate from light (u, d, s) quarks and gluons (W+light jets). Depending on the jet multiplicity the W+jets events contain heavy flavor jets resulting from gluon splitting into $b\bar{b}$ or $c\bar{c}$ ($Wb\bar{b}$ or $Wc\bar{c}$, respectively). A sizable background arises from production of two or more jets ("multijets"), with one of the jets misidentified as a lepton and accompanied by large $\not\!\!E_T$ resulting from mismeasurements of jet energies. Significantly smaller contributions to the selected sample arise from single top, Z+jets, and weak diboson (WW, WZ and ZZ) production. The smaller backgrounds are referred to as "other" backgrounds.

The normalization of the various backgrounds starts by the determination of the number of multijet events in the selected sample. The multijet background is determined using control samples from data and probabilities for jets to mimic isolated lepton signatures also determined from data [9]. This method allows to determine the fraction of events with a real isolated high p_T lepton ($t\bar{t}$ and all backgrounds except multijet background) and the fraction of events from the multijet background. The contribution from single top, Z+jets and weak diboson production are determined from Monte Carlo simulation, where we use the theoretical NLO cross sections [10] and the selection efficiency from the Monte Carlo. The remainder of the selected sample is either $t\bar{t}$ or W+jets production. Since tagging probabilities for $t\bar{t}$ events and W+jets are different, both the $t\bar{t}$ and the W+jets absolute contributions are allowed to vary when we fit $\mathcal{B}(t \to Wb)/\mathcal{B}(t \to Wq)$ and $\sigma_{t\bar{t}}$ to the data. The diboson samples were generated with PYTHIA [12], Z+jets and W+jets with ALPGEN [13].The single top background was simulated with CompHEP [14]. The signal samples were generated with PYTHIA [12] including three decay modes $t\bar{t} \to W^+b\ W^-\bar{b}$, $t\bar{t} \to W^+b\ W^-\bar{q}_\ell$ and $t\bar{t} \to W^+q_\ell\ W^-\bar{q}_\ell$ where q_ℓ denotes a light quark.

IV. LIFETIME-TAGGING

The measurement is based on the identification of b-quark jets. For this purpose we use a b-tagging algorithm, based on a neural network. The calculation of the event tagging probability used to separate the sample in 0, 1 and 2 tagged events is described in [18].

A. $\mathbf{t\bar{t}}$ Event Tagging Probability for $\mathcal{B}(\mathbf{t \to Wb})/\mathcal{B}(\mathbf{t \to Wq}) \neq 1$

In the standard model case with $\mathcal{B}(t \to Wb)/\mathcal{B}(t \to Wq) = 1$ the $t\bar{t}$ event tagging probabilities are computed assuming that each of the signal events contains two b-jets. In the present analysis the $t\bar{t}$ event tagging probability becomes a function of $\mathcal{B}(t \to Wb)/\mathcal{B}(t \to Wq)$. In general, for $R \neq 1$, a $t\bar{t}$ event might have 0, 1 or 2 b-jets from the two top quark decays, strongly affecting the event tagging probability and how $t\bar{t}$ events are distributed among the zero-, single- and double-tag samples. To derive the $t\bar{t}$ event tagging probability as function of R we determine the event tagging probability for the three following scenarios:

1. $t\bar{t} \to W^+b\ W^-\bar{b}$ (referred to as $tt \to bb$);
2. $t\bar{t} \to W^+b\ W^-\bar{q}_\ell$ or its charge conjugate (referred to as $tt \to bq_\ell$);
3. $t\bar{t} \to W^+q_\ell\ W^-\bar{q}_\ell$ (referred to as $tt \to q_\ell q_\ell$),

where q_ℓ denotes either a d- or a s-quark. The probabilities $P_{\mathrm{n-tag}}$ to observe $\mathrm{n-tag} = 0$, 1 or ≥ 2 lifetime-tagged jets are computed from Monte Carlo simulation separately for the three types of $t\bar{t}$ events using the b-tagging efficiency for b-jets, efficiency to tag a c-jet and probability to tag a light flavor jet as b-jet. Tagging efficiencies for different jet flavors are tuned in simulation to reproduce the tagging rates observed in data. The probabilities $P_{\mathrm{n-tag}}$ in the three scenarios are then combined in the following way to obtain the $t\bar{t}$ tagging probability as function of R:

$$P_{\mathrm{n-tag}}(tt) = R^2 P_{\mathrm{n-tag}}(tt \to bb) + 2R(1-R)P_{\mathrm{n-tag}}(tt \to bq_\ell) + (1-R)^2 P_{\mathrm{n-tag}}(tt \to q_\ell q_\ell), \quad (2)$$

where the subscript $\mathrm{n-tag}$ runs over 0, 1 and ≥ 2 tags. An example for the event tagging fractions as a function of R is shown in Fig. 1 for the electron channel and at least four jets. The fractions look similar for the different channels.

V. TOPOLOGICAL DISCRIMINANT IN THE ZERO-TAG SAMPLE

To better constrain the number of $t\bar{t}$ events in the ℓ+4 jets zero-tag sample we use a topological discriminant function that makes use of the differences between the kinematic properties of the $t\bar{t}$ events and the backgrounds. We

selected different variables, well modeled by simulation in low jet multiplicity samples with negligible top contribution, providing good separation between signal and W+jets background. To reduce the dependence on modeling of soft radiation and underlying event, only the four highest p_T jets were used to determine these variables. The discriminant function in the electron channel is built from the following variables:

Aplanarity: The Aplanarity A is defined as $\mathcal{A} = \frac{3}{2}\lambda_3$, where λ_3 is the smallest eigenvalue of the normalized momentum tensor $\mathcal{M}$ [15].

$\mathcal{C}_{\mathbf{M}}$**:** The variable $\mathcal{C}_M$ is defined here as $3(\lambda_1\lambda_2+\lambda_1\lambda_3+\lambda_2\lambda_3)$ where λ_1, λ_2 and λ_3 are the eigenvalues of the normalized momentum tensor $\mathcal{M}$.

D_M**:** The variable D_M is defined as $27\lambda_1\lambda_2\lambda_3$ with λ_1, λ_2 and λ_3 being the eigenvalues of the normalized momentum tensor $\mathcal{M}$.

Leading jet p_T**:** The p_T of the jet with the highest p_T in an event.

$\mathbf{\Delta R_{max}}$**:** ΔR_{max} is the maximal ΔR between two of the four leading jets in the event.

In the muon channel, in addition to Aplanarity and $\mathcal{D}_M$, the following variables are used:

$\mathbf{H_T^l}$**:** H_T^l is defined as the scalar sum of p_T of the four leading jets in an event and the p_T of the lepton from W decay.

$\mathbf{H_T3}$**:** H_T3 is defined as the scalar sum of the p_T of the third and fourth jet in an event.

$\mathbf{M_T^{jet}}$**:** The variable M_T^{jet} is defined as the transverse mass of the vector sum of all four leading jets in the event.

$\mathbf{M_{012}/M_{all}}$**:** this variable is defined as the mass of the three leading jets divided by the mass of the event. The mass of the event is defined as the invariant mass of the vector sum of all four jets, the lepton from W decay and the reconstructed neutrino.

The discriminant function was built using the method described in [17], and has the following general form:

$$\mathcal{D} \;=\; \frac{S(x_1, x_2, ...)}{S(x_1, x_2, ...) + B(x_1, x_2, ...)}\,, \tag{3}$$

where $x_1, x_2, ...$ is a set of input variables and $S(x_1, x_2, ...)$ and $B(x_1, x_2, ...)$ are the probability density functions for the $t\bar{t}$ signal and background, respectively. Neglecting the correlations between the input variables, the discriminant function can be approximated by the expression:

$$\mathcal{D} \;=\; \frac{\prod_i s_i(x_i)/b_i(x_i)}{\prod_i s_i(x_i)/b_i(x_i) + 1}\,, \tag{4}$$

where $s_i(x_i)$ and $b_i(x_i)$ are the normalized distributions of variable i for signal and background, respectively. As constructed, the discriminant function peaks near zero for the background, and near unity for the signal. The shape of the discriminant $\mathcal{D}$ is derived from simulated $t\bar{t}$ and W+jets events. For the $t\bar{t}$ events the differences in shape for the three different decays $tt \to bb$, $tt \to bq_\ell$ and $tt \to q_\ell q_\ell$ are taken into account. For the multijet background the discriminant shape is obtained by applying the discriminant function to a sample of data events selected by requiring that the leptons fail the tightest lepton isolation criteria while passing the loose ones (referred to as loose–tight sample). The other backgrounds have kinematic properties similar to the W+jets events. They are assumed to have the same discriminant shape as the W+jets events. The comparison of shapes for $tt \to bb$, W+jets and multijet events is presented in Fig. 2.

VI. TOTAL DEPENDENCE ON R

To improve the method of the previous analysis [4] we take into account two more dependencies on R: the dependence of the preselection efficiency and the topological discriminant shape on R. For the extraction of R we thus take into account three effects: the $t\bar{t}$ event tagging probability depends on R as described in section IV A, the preselection efficiency also depends on R and the shape of the topological discriminant depends on the $t\bar{t}$ decay mode.

The preselection efficiency depends on R in the same way as the tagging probability. The combined preselection and event tagging probability result in

$$P_{total}(t\bar{t}) = R^2 P_p(t\bar{t} \to b\bar{b}) P_b(t\bar{t} \to b\bar{b}) + 2R(1-R) P_p(t\bar{t} \to b\bar{q_\ell}) P_b(t\bar{t} \to b\bar{q_\ell}) + (1-R)^2 P_p(t\bar{t} \to q_\ell\bar{q_\ell}) P_b(t\bar{t} \to q_\ell\bar{q_\ell}), \tag{5}$$

with P_b describing the tagging probability and P_p the preselection efficiency for a certain process. The topological discriminant depends slightly on the $t\bar{t}$ decay. It is more pronounced for the muon channel as can be seen from the bottom plots in Fig. 2.

VII. RESULTS

To measure $\mathcal{B}(t \to Wb)/\mathcal{B}(t \to Wq)$ and $\sigma_{t\bar{t}}$ we perform a binned maximum likelihood fit to the data. The data are binned in: *i*) ten bins of the discriminant $\mathcal{D}$ in e + 4 jets zero-tag events, *ii*) ten bins of the discriminant $\mathcal{D}$ in μ + 4 jets zero-tag events, *iii*) two bins for the two zero-tag samples e+ 3 jets, μ+3 jets, *iv*) four bins for the four single-tag samples (electron or muon and 3 or 4 jets), *v*) four bins for the four double-tag samples (electron or muon and 3 or 4 jets). In each bin we make a prediction on the number of events which is the sum of the expected background and the signal contribution. The signal contribution is a function of R and $\sigma_{t\bar{t}}$. To predict the number of events in each bin of the discriminant $\mathcal{D}$ we use its expected shape for the backgrounds and the three different $t\bar{t}$ signal samples. The normalization of the multijet background is estimated by counting events in loose–tight samples. The number of events in each such sample is allowed to fluctuate statistically. We therefore use an additional bin in the likelihood fit to take into account statistical fluctuations in the multijet background calculation. This results in a likelihood function that is the product of 30 Poisson terms in the signal bins *i*) to *v*) and 12 Poisson terms in the twelve bins accounting for statistical fluctuations of multijet background in zero-tag, single-tag and double-tag events with 3 or 4 jets and for e + jets and μ + jets. We incorporate systematic uncertainties into the likelihood by using nuisance parameters [19]. All preselection efficiencies, tagging probabilities and shapes of the discriminant $\mathcal{D}$ become functions of the nuisance parameters. The final likelihood function contains one Gaussian term for each nuisance parameter. The values of $\mathcal{B}(t \to Wb)/\mathcal{B}(t \to Wq)$ and $\sigma_{t\bar{t}}$ that maximize the total likelihood function are measured to be:

$$\begin{aligned} R &= 0.991^{+0.094}_{-0.085}\ \text{(stat+syst)}\ , \\ \sigma(t\bar{t}) &= 8.10^{+0.87}_{-0.82}\ \text{(stat+syst)} \pm 0.49\ \text{(luminosity)\ pb}\ , \end{aligned}$$

in good agreement with the standard model expectation of $R = 1$ and $\sigma_{t\bar{t}} = 6.8 \pm 0.6$ [20] for the top quark mass of 175 GeV. The statistical and dominant systematic uncertainties and their contributions to the total uncertainties are given in Tables 1 and 2. The result of the 2-dimensional fit is shown in the plane ($\mathcal{B}(t \to Wb)/\mathcal{B}(t \to Wq)$, $\sigma_{t\bar{t}}$) in Figure 3, along with the 68% and 95% confidence level contours.

Figure 4 shows the comparison of the number of events with 0, 1 and at least 2 tags observed in data with the sum of predicted background and measured signal for $R = 1$. Predicted and observed number of events in the 0-tag sample in bins of the topological discriminant is presented in Figure 5.

In addition to a simultaneous measurement we fixed R to one and measured $\sigma_{t\bar{t}}$ with the same likelihood maximization procedure. This results in

$$\sigma(t\bar{t}) = 8.08^{+0.85}_{-0.80}\ \text{(stat+syst)} \pm 0.49\ \text{(lumi)\ pb.}$$

For the events with at least four jets the cross section is measured to be

$$\sigma(t\bar{t}) = 8.27^{+0.96}_{-0.95}\ \text{(stat+syst)} \pm 0.51\ \text{(lumi)\ pb.}$$

Figure 7 shows a summary of the R measurements performed at the Tevatron.

We also extract lower limits on R and the CKM matrix element $|V_{tb}|$. For the limit extraction procedure the likelihood ordering principle according to Feldman-Cousins [3, 21] is used. To determine the limits we generate ensembles for various input values R_{true} taking into account all systematic uncertainties. Figure 6 shows the bands of 99%, 95% and 68% C. L. for R_{true} as a function of the measured quantity R_{meas}. We obtain $R > 0.904$ at 68% C.L. and $R > 0.812$ at 95% C.L.. The limits on $|V_{tb}|$ can be extracted assuming $|V_{tb}| = \sqrt{R}$ or by resolving Eq. 1 for $|V_{tb}|$ directly [23]. For the latter we do not use the assumption of a unitary CKM matrix or three generations of quarks but only insert the measured values of $|V_{ts}|$ and $|V_{td}|$ given in [1]. For $|V_{tb}|$ we obtain $|V_{tb}| > 0.950$ at 68% C.L. and $|V_{tb}| > 0.901$ at 95% C.L with assuming a unitary CKM matrix and $|V_{tb}| > 0.096$ at 95% C.L. without assumptions on the CKM matrix. Ref. [22] quotes a lower limit of $|V_{tb}| > 0.07$ at 90% C.L. for the existence of more than three quark generations.

Acknowledgments

We thank the staffs at Fermilab and collaborating institutions, and acknowledge support from the DOE and NSF (USA); CEA and CNRS/IN2P3 (France); FASI, Rosatom and RFBR (Russia); CAPES, CNPq, FAPERJ, FAPESP and FUNDUNESP (Brazil); DAE and DST (India); Colciencias (Colombia); CONACyT (Mexico); KRF and KOSEF (Korea); CONICET and UBACyT (Argentina); FOM (The Netherlands); Science and Technology Facilities Council (United Kingdom); MSMT and GACR (Czech Republic); CRC Program, CFI, NSERC and WestGrid Project (Canada); BMBF and DFG (Germany); SFI (Ireland); The Swedish Research Council (Sweden); CAS and CNSF (China); Alexander von Humboldt Foundation; and the Marie Curie Program.

Source	Uncertainty on $\mathcal{B}(t \to Wb)/\mathcal{B}(t \to Wq)$
Statistical	$+0.066\ -0.064$
b-tagging efficiency	$+0.063\ -0.049$
Uncertainty on multijet background	$+0.017\ -0.017$
Others	$+0.016\ -0.021$
Total error	$+0.094\ -0.085$

TABLE 1: *Statistical and systematic uncertainties on $\mathcal{B}(t \to Wb)/\mathcal{B}(t \to Wq)$ in units of $\mathcal{B}(t \to Wb)/\mathcal{B}(t \to Wq)$. Only the major systematic uncertainties are listed separately.*

Source	Uncertainty on $\sigma_{t\bar{t}}$ (pb)
Statistical	$+0.65\ -0.62$
Lepton identification and trigger	$+0.36\ -0.33$
Jet energy scale	± 0.24
b-tagging efficiency	$+0.14\ -0.12$
Flavor composition of W+jets background	$+0.23\ -0.22$
Uncertainty on multijet background	$+0.18\ -0.17$
Others	$+0.21\ -0.17$
Total error	$+0.87\ -0.82$

TABLE 2: *Statistical and systematic uncertainties on $\sigma_{t\bar{t}}$ in pb. Only the major systematic uncertainties are listed separately.*

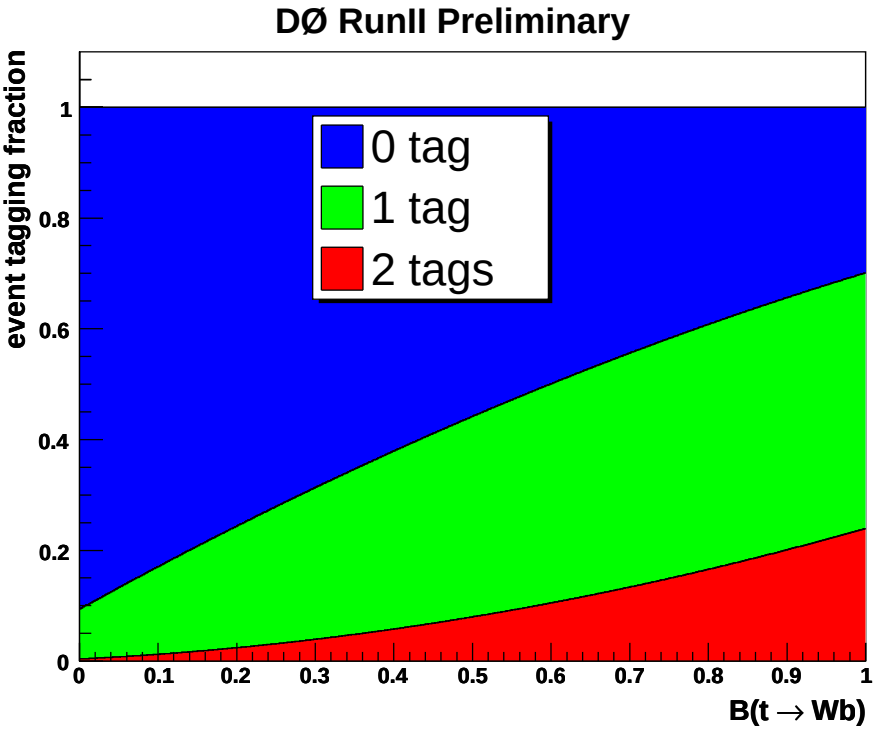

FIG. 1: *Fractions of events with 0-, 1- and 2 or more tags as function of R for the electron channel and at least four jets.*

(a)

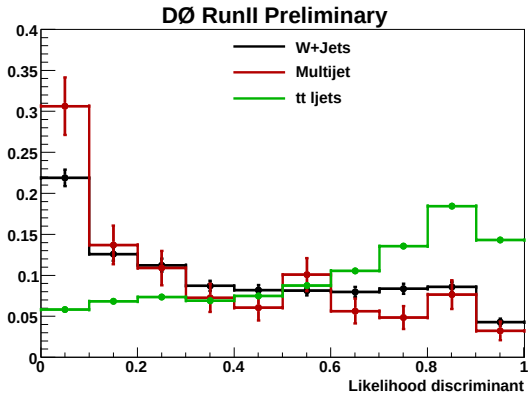

(b)

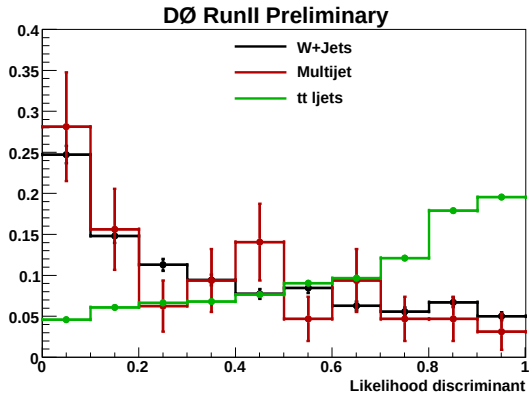

(c)

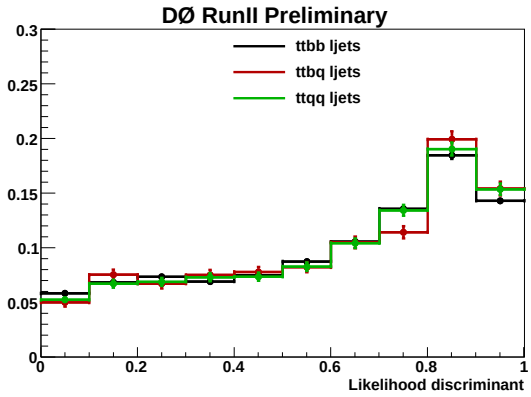

(d)

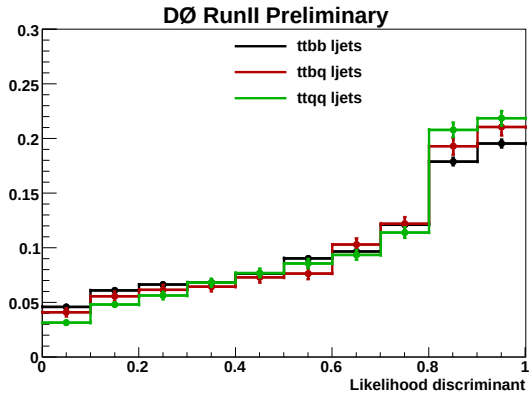

FIG. 2: *(a), (b): Topological discriminant templates in the (a) electron and (b) muon channel for* $t\bar{t} \to WbWb$*, W+jets and multijet events. (c), (d): Topological discriminant templates in the (c) electron and (d) muon channel for* $t\bar{t} \to WbWb$*,* $t\bar{t} \to WbWq$ *and* $t\bar{t} \to WqWq$*.*

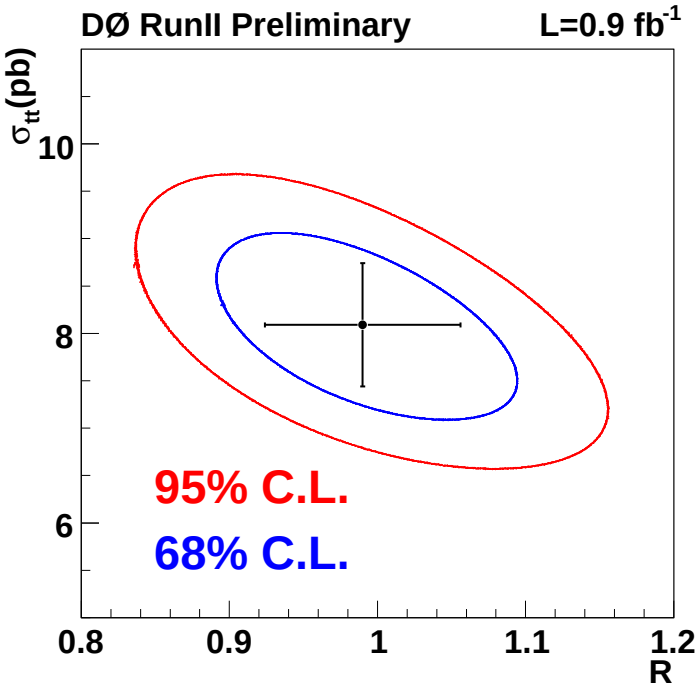

FIG. 3: *The 68% and 95% C.L. contours in the plane* $(\mathcal{B}(t \to Wb)/\mathcal{B}(t \to Wq), \sigma_{t\bar{t}})$ *using statistical uncertainties only. The point indicates the best fit to data.*

(e3)

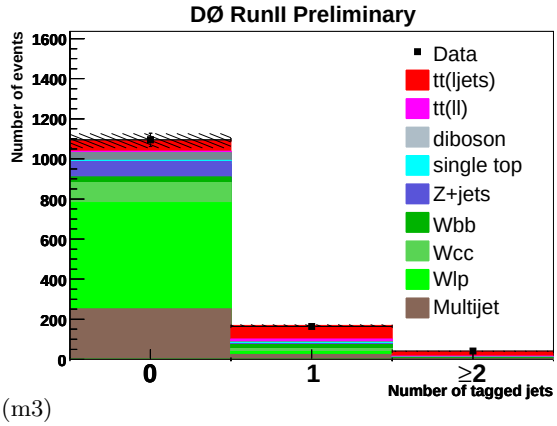

(e4)

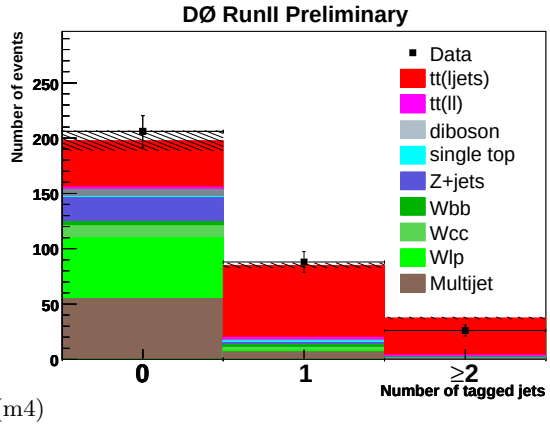

(m3)

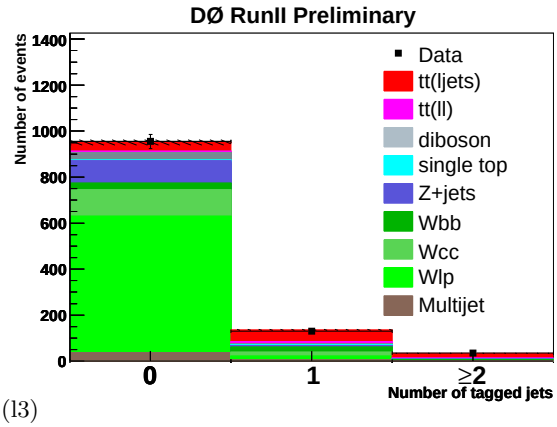

(m4)

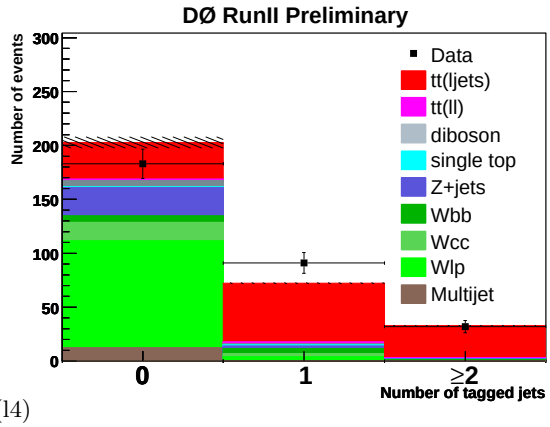

(l3)

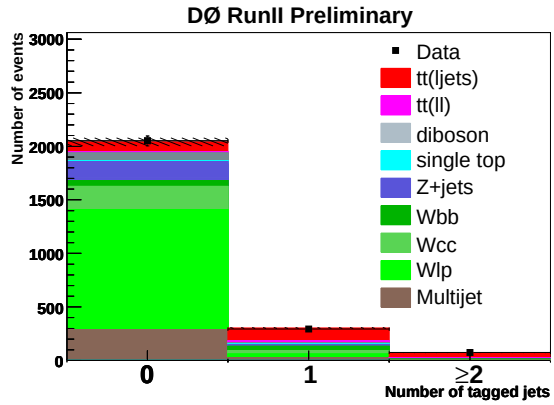

(l4)

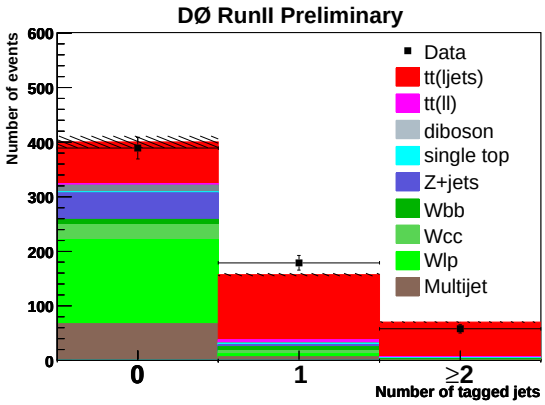

FIG. 4: *Predicted and observed number of events in the the zero-, single- and double-tag samples for $R = 1$ and $\sigma_{t\bar{t}} = 8.1$ pb measured in this analysis for electron channel (e3, e4), muon channel (m3,m4) and combined (l3,l4) for events with exactly three jets (e3,m3,l3) and at least four jets (e4,m4,l4).*

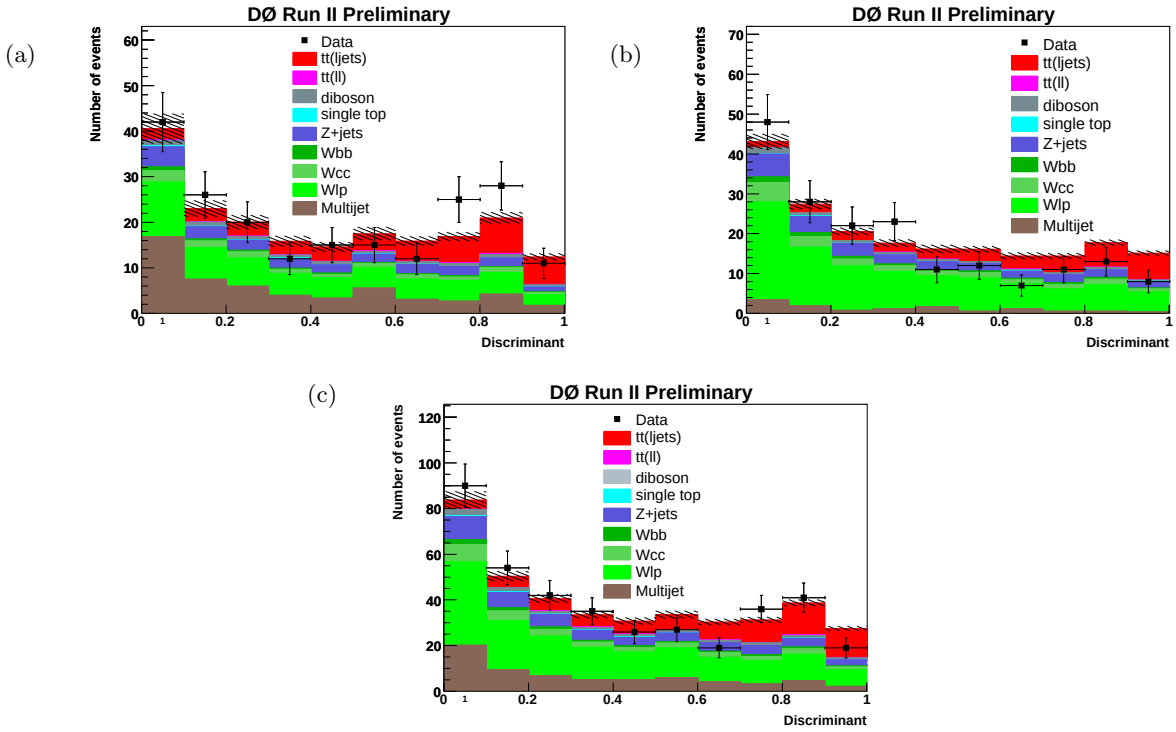

FIG. 5: *Predicted and observed number of events in the in the zero-tag sample in bins of topological discriminant for $R = 1$ and $\sigma_{t\bar{t}} = 8.1$ pb measured in this analysis for (a) electron channel, (b) muon channel and (c) combined.*

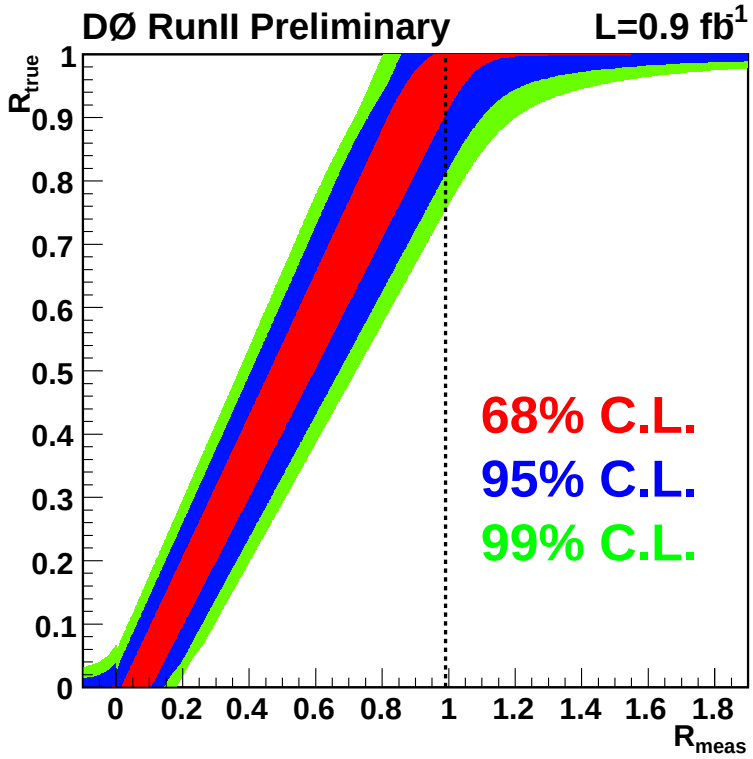

FIG. 6: *The 68% (inner band), 95% (middle band) and 99% (outer band) C.L. bands for R_{true} as a function of R_{meas}. The dotted black line indicates the measured value $R = 0.991$.*

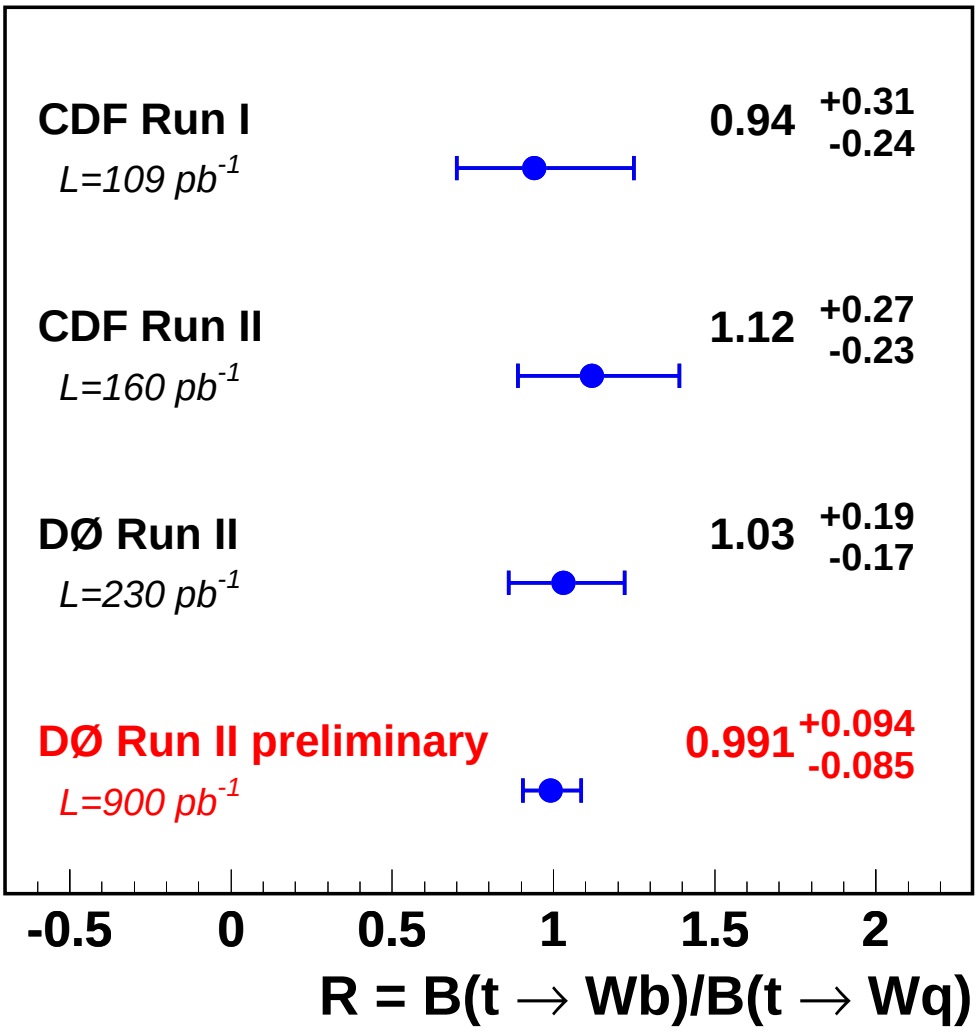

FIG. 7: *Summary of R measurements at the Tevatron.*

[1] W. M. Yao *et al.*, Journal of Physics G **33**, 1 (2006).
[2] CDF Collaboration, T. Affolder *et al.*, Phys. Rev. Lett. **86**, 3233 (2001).
[3] CDF Collaboration, T. Affolder *et al.*, Phys. Rev. Lett., **95**, 102002 (2005).
[4] DØ Collaboration, V. Abazov *et al.*, Phys. Lett. B **639**, 616 (2006).
[5] DØ Collaboration, V. Abazov *et al.*, Nucl. Instrum. and Methods Phys. Res. A **565**, 463 (2006).
[6] Rapidity y and pseudorapidity η are defined as functions of the polar angle θ and parameter β as $y(\theta,\beta) \equiv \frac{1}{2}\ln\left[(1+\beta\cos\theta)/(1-\beta\cos\theta)\right]$ and $\eta(\theta) \equiv y(\theta,1)$, where β is the ratio of a particle's momentum to its energy.
[7] Impact parameter is defined as the distance of closest approach (d_{ca}) of the track to the primary vertex in the plane transverse to the beamline. Impact parameter significance is defined as $d_{ca}/\sigma_{d_{ca}}$, where $\sigma_{d_{ca}}$ is the uncertainty on d_{ca}.
[8] V. Abazov *et al.*, FERMILAB-PUB-05-034-E (2005).
[9] DØ Collaboration, V. Abazov *et al.*, Phys. Lett. B **626**, 45 (2005).
[10] Z. Sullivan, Phys. Rev. D **70**, 114012 (2004); J.M. Campbell and R.K. Ellis, Phys. Rev. D **60**, 113006 (1990).
[11] We use the iterative, seed-based cone algorithm including midpoints, as described on p. 47 in G. C. Blazey *et al.* , in Proceedings of the Workshop: *"QCD and Weak Boson Physics in Run II",* edited by U. Baur, R. K. Ellis, and D. Zeppenfeld, FERMILAB-PUB-00-297 (2000).
[12] T. Sjöstrand, L. Lonnblad, S. Mrenna, PYTHIA 6.3: Physics and manual, hep-ph/0308153(2003).
[13] M. L. Mangano et al, ALPGEN, a Generator for Hard Multiparton Processes in Hadron Collisions, CERN-TH-2002-129, FTN-T-2002-06, hep-ph/0206293(2002).
[14] E.E. Boos et al., Method for simulating electroweak top-quark production events in the NLO approximation: Single Top event generator, Phys. Atom. Nucl. **69**, 1317 (2006).
[15] The normalized momentum tensor $\mathcal{M}$ is defined as

$$\mathcal{M}_{ij} = \frac{\Sigma_o p_i^o p_j^o}{\Sigma_o |\vec{p^o}|^2},$$

where $\vec{p^o}$ is the momentum vector of a reconstructed object o, and i and j are Cartesian coordinates. A more precise description is given in [16].
[16] V. Barger, J. Ohnemus, and R.J.N. Phillips, Phys. Rev. D **48**, 3953 (1993).
[17] DØ Collaboration, B. Abbott *et al.*, Phys. Rev. D **58**, 052001 (1998).
[18] T. Scanlon, Ph.D. thesis, University of London, 2006. FERMILAB-THESIS-2006-43.
[19] P. Sinervo, in *Proceedings of Statistical methods in Particle Physics, Astrophysics, and Cosmology*, edited by L. Lyons, R. P. Mount, and R. Reitmeyer (SLAC, Stanford, 2003), p. 334.
[20] N. Kidonakis and R. Vogt, Phys. Rev. D **68**, 114014 (2003) and private communication.
[21] G. Feldman and R. Cousins, Phys. Rev. D **57**, 3873 (1998).
[22] Equation (11.14) in S. Eidelman et al., Phys. Lett., B **592**, 1 (2004).
[23] In both cases we neglect the dependence of the single top background on $|V_{tb}|$ since its contribution is very small.